Excitation properties of hydrogen-related photoluminescence in 6*H*-SiC

T. Egilsson, A. Henry, I. G. Ivanov, A. Ellison, and E. Janzén
Department of Physics and Measurement Technology, Linköping University, S-581 83 Linköping, Sweden
(Received 9 July 1999)

We have studied the excitation properties of a well-known hydrogen-related bound exciton (H-BE) photoluminescence (PL) in 6*H*-SiC. In the case of the so-called primary H-BE's, photoluminescence excitation (PLE) spectroscopy reveals several excited states that have not been reported previously. In order to explain these states we propose a pseudodonor model. The primary H-BE's are thus regarded as donors where strongly localized holes serve as the positive cores. From a comparison between the PLE spectra of the three different primary H-BE's corresponding to the three inequivalent substitutional lattice sites in 6*H*-SiC, we attempt to distinguish between the hexagonal and cubic lattice sites. We have also investigated the dependence of the optically induced quenching of the H-BE PL on the energy of the exciting light. We observe that the quenching of the H-BE PL is only efficient when the exciting light has energy above the threshold for phonon-assisted free-exciton (FE) formation or when its energy coincides with the energy needed for resonant absorption into the H-BE states. When creating FE's, we observe different types of behavior depending on the initial conditions. We argue that our results are best explained by the existence of two configurations of the same charge state of the H defect, namely a stable one: *A* (giving rise to the H-BE PL), and a metastable one: *B* (not revealed in the PL spectrum). The recombination of excitons bound at these two configurations can give rise to the transformations $A \rightarrow B$ and $B \rightarrow A$. The existence of the *B* configuration is revealed through the effect of the $B \rightarrow A$ process on the temporal changes of the H-BE PL.

I. INTRODUCTION

In the early 1970s, Choyke and Patrick (Ref. 1) reported strong bound exciton (BE) photoluminescence (PL) spectra in silicon carbide (SiC) implanted with the hydrogen isotopes H (^{1}H) and D (^{2}H). The PL spectra in the case of H and D implantation are very similar apart from the energy positions of some prominent lines in the phonon-assisted sidebands. The energy displacements of these lines from the no-phonon lines, approximately 370 meV in H-implanted and 274 meV in D-implanted SiC, correspond to the energies of C-H and C-D bond-stretching vibrational modes, respectively.[1] This confirmed the involvement of the implanted species (H or D) in the optical centers. The defect was proposed to consist of an H or D atom bonded to one of the four C atoms neighboring a Si vacancy.[2] In recent years the H-related PL has also been observed in SiC layers grown by chemical vapor deposition.[3] In the following we will refer to these defects as H and D defects, the excitons bound to them as H-and D-BE's, and the PL due to the BE recombination as H- and D-PL. An interesting feature of the H-PL spectrum is the quenching of the PL intensity under prolonged optical excitation at low temperatures.[4,5] The original PL intensity at low temperature can be restored by annealing at room temperature.[4,5] No such quenching is observed in the case of the D-PL.[4] In order to explain this behavior, Dean and Choyke (Ref. 6) proposed a recombination-enhanced defect reaction (REDR). In this model one recognizes the fact that a part of the H-BE recombination energy may be channeled into vibrational motion of the defect atoms. This local vibrational energy may be sufficient to overcome the potential barrier for transfer of the light H atom to a neighboring site, thereby dissociating the defect. The vibrational energy is smaller when H is replaced by D and is apparently not sufficient for dissociating the defect.

H-PL spectra have been observed in 4*H*-, 6*H*-, and 15*R*-SiC,[2,4,7] but not in the cubic polytype 3*C*-SiC.[2] In 6*H*-SiC, the H-PL spectrum contains lines of two types called primary and secondary, whereas in 4*H*- and 15*R*-SiC only lines of the primary type are observed. Replicas associated with the C-H local modes are observed only in the case of the primary PL lines. However, since the secondary PL lines observed in 6*H*-SiC depend on annealing in the same way as the primary PL lines, it has been claimed that both types of lines are due to the same defect.[8] In this paper we will be concerned only with the 6*H* polytype.

Figure 1 shows the no-phonon part of a typical H-BE PL spectrum in 6*H*-SiC. The H_1, H_2, and H_3 lines are no-phonon lines associated with the primary H-BE's, whereas the H_4, H_5, and H_{5F} are no-phonon lines associated with secondary H-BE's. The inset shows the C-H mode replicas of the primary lines. Also visible in the spectrum are the *R* and *S* no-phonon lines associated with BE's at nitrogen donors (N-BE's). The peaks labeled ''?'' in the figure are of unknown origin. Figure 2 shows the energy positions of all previously reported H-BE states in 6*H*-SiC, as well as those reported in this paper (H_{1T}, H_{2T}, and $\alpha_3, \beta_3, \gamma_3, \delta_3, \varepsilon_3, \zeta_3, \eta_3$). The energy values are listed in Table I. In 6*H*-SiC, the crystal structure is such that there are three inequivalent substitutional lattice sites, and thus three inequivalent silicon vacancies. The energies of the H-BE's associated with the different sites are not the same. The indices 1, 2, and 3 refer to the three different sites in the case of the primary H-BE's, but for the secondary H-BE's the sites are labeled 4 and 5. The reason for the observation of only two, instead of three, secondary H-BE's is not known but might be due according to Ref. 5 to the exciton not being bound at one of the sites. At 1.3 K only transitions from the

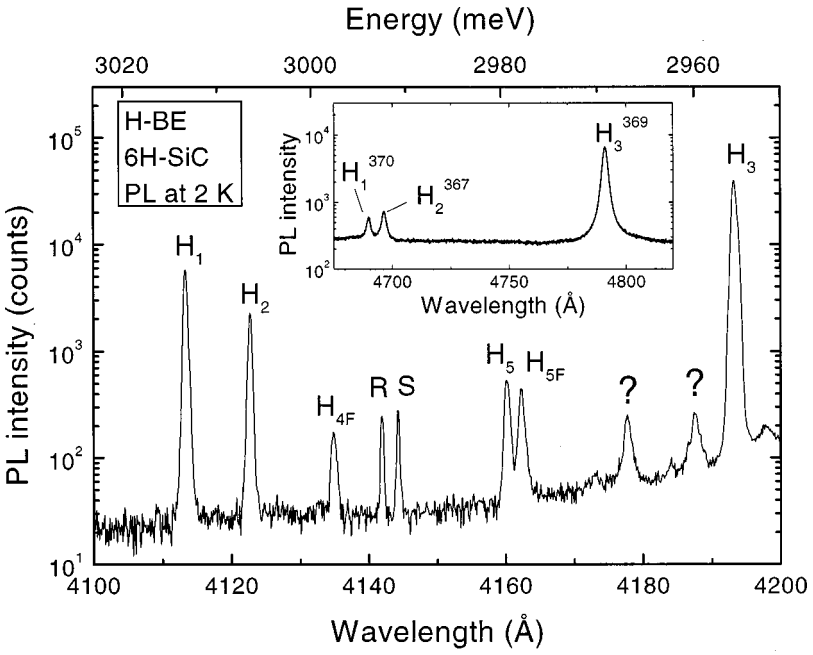

FIG. 1. The no-phonon part of a typical H-BE PL spectrum in 6*H*-SiC. The spectrum was recorded at 2 K. The H_1, H_2, and H_3 lines are no-phonon lines associated with the primary H-BE's, whereas the H_4, H_5, and H_{5F} are no-phonon lines associated with secondary H-BE's. The inset shows the C-H vibrational mode replicas at approximately 370 meV below the primary no-phonon lines. Also visible in the spectrum are the *R* and *S* no-phonon lines associated with BE's at nitrogen donors at the two cubic lattice sites in 6*H*-SiC (the *P* line associated with the hexagonal site N-BE is buried under the H_2 line). The peaks labeled ''?'' in the figure are of unknown origin.

lowest-energy states of the H-BE's are observed in the PL spectrum, i.e., the H_1, H_2, H_3, H_{4F}, and H_{5F} no-phonon lines.[2] In PL spectra recorded at higher temperatures, no-phonon lines associated with the H_4, H_5, H_{3T}, and H_{5T} states have been observed.[2,5] Already at 2 K the H_5 no-phonon line is observed (see Fig. 1). High-resolution PL measurements have shown that the no-phonon lines at low temperature in both the primary and secondary spectra are composed of two closely spaced components[5,8] (these are not resolved in the spectrum shown in Fig. 1). This has been explained by the difference between nonaxial (NA) and axial (*A*) C-H bonds in the uniaxial 6*H*-SiC crystal.[5] The splitting is exemplified in the blown-up view of the H_3 line in Fig. 2. The spacing between the two components ranges from 0.17 to 0.37 meV for the different lines and their intensity ratio is between $\frac{1}{3}$ and $\frac{1}{5}$ (NA being the stronger component).[5]

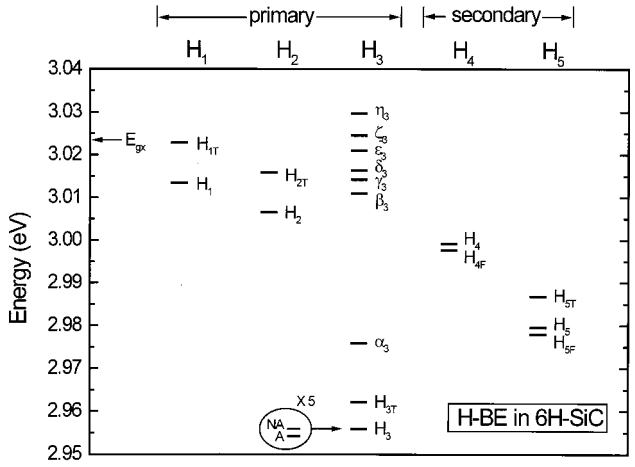

FIG. 2. Energy positions of all previously reported H-BE states in 6*H*-SiC, as well as those reported in this paper (H_{1T}, H_{2T}, and $\alpha_3, \beta_3, \gamma_3, \delta_3, \varepsilon_3, \zeta_3, \eta_3$). The H-BE's are of two kinds, primary and secondary. The different H-BE's within each group are associated with inequivalent lattice sites in 6*H*-SiC.

In this paper we report the excitation properties of the H-BE photoluminescence in 6*H*-SiC. PL excitation (PLE) spectroscopy reveals several excited states of the primary H-BE's which have not been reported previously. A pseudo-donor model (BE at a hole attractive isoelectronic defect) is proposed in order to explain the electronic structure of the primary H-BE's. From the dependence of the quenching of the H-PL on the excitation energy, we propose that the H defect has two configurations, a stable one: *A* (giving rise to the H-PL), and a metastable one: *B* (not giving rise to PL). The paper is organized as follows: (i) In Sec. II we describe the experimental details; (ii) the PLE results and their interpretation are given in Sec. III A and III B; (iii) Secs. III C and III D present and discuss the results concerning the excitation dependence of the H-PL quenching; (iv) finally in Sec. IV we give a summary.

II. EXPERIMENT

The sample used for this investigation was a 180-μm-thick 6*H*-SiC layer grown by high-temperature chemical va-

TABLE I. Energy positions of all the H-BE states in 6*H*-SiC observed in this work (the H_{1T}, H_{2T}, and $\alpha_3, \beta_3, \gamma_3, \delta_3, \varepsilon_3, \zeta_3, \eta_3$ states have not been observed previously). Apart from the absolute energies, the table lists also the energy of the states with respect to the lowest-energy state of each H-BE.

Label	Energy (eV)	$\Delta E/H_3$ (meV)	Label	Energy (eV)	$\Delta E/H_{1,2,4F,5F}$ (meV)
H_3	2.9559	0	H_1	3.0134	0
H_{3T}	2.9621	6.2	H_{1T}	3.0228	9.4
α_3	2.9759	20.0	H_2	3.0065	0
β_3	3.0109	55.0	H_{2T}	3.0159	9.4
γ_3	3.0142	58.3	H_{4F}	2.9977	0
δ_3	3.0163	60.4	H_4	2.9991	1.4
ε_3	3.0210	65.1	H_{5F}	2.9779	0
ζ_3	3.0245	68.6	H_5	2.9795	1.6
η_3	3.0296	73.7	H_{5T}	2.9868	8.9

por deposition (HTCVD). The growth was carried out on the Si face of an *n*-type ($2\times10^{18}\,\mathrm{cm}^{-3}$) on-axis 6*H*-SiC substrate at slightly above 2200 °C. The incorporation of hydrogen into the layer occurred unintentionally during growth.

For the optical experiments the sample was cooled in a He bath cryostat. For PLE spectroscopy a tunable dye laser pumped with the multiline UV output of an Ar^+-ion laser was used as an excitation source. The luminescence was spectrally resolved by a 0.85-m SPEX 1404 double grating monochromator fitted with 1800 grooves/mm gratings, and detected by a Hamamatsu photomultiplier tube (PMT) operating in photon counting mode.

III. RESULTS

A. PLE spectra

The H-BE PLE spectra were measured by detecting the H-PL at a particular no-phonon line or phonon replica at 2 K while scanning the excitation energy. PLE spectra corresponding to the H_1, H_2, H_3, H_5, and H_{5F} no-phonon lines as well as a couple of H_3 phonon replicas were obtained. The PL lines associated with the H_4 BE were, on the other hand, too weak to enable reliable PLE measurements. The resolution at the detection side in these measurements was approximately 0.6 meV, and the detected signal therefore contained a contribution from both the NA and *A* components of the lines. Since the detection energy is close to the excitation energy in the PLE experiments (usually within the phonon energy region), lines due to Raman scattering may overlap with the spectra. When scanning the laser excitation, the Raman spectrum follows the laser line, so each time the energy separation between the detection energy and excitation energy coincides with the energy of a Raman mode, a peak will appear in the PLE spectrum. Since the Raman peaks do not depend on the PL, they are observed irrespective of whether the detection energy coincides with the energy of a PL transition or not. They are thus easily identified by comparing excitation spectra corresponding to different detection energies.

The PLE spectra detected at the H_1, H_2, and H_5 no-phonon lines are shown in Figs. 3(a)–3(c), respectively. The upper energy limits of the three spectra correspond to absolute energies just below the onset of the phonon-assisted free-exciton (FE) absorption [FE absorption edge (FEAE)]. Above the FEAE it is very difficult to distinguish any H-BE PLE peaks from the large background due to FE absorption. The PLE spectrum of the H_{5F} line is identical to the H_5 PLE spectrum and is thus not shown. The polarization of the exciting light was $\bar{E}\perp\bar{c}$, where $\bar{c}$ denotes the crystal axis (*c* axis) of 6*H*-SiC, and $\bar{E}$ the electric field vector of the light. The PLE peaks in Fig. 3 are labeled H_{1T}, H_{2T}, and H_{5T}. Other peaks in the spectra are Raman peaks. In particular, the three Raman peaks labeled R_1^{el}, R_2^{el}, and R_3^{el} are due to electronic Raman scattering associated with nitrogen donors,[9] of which there is a rather high concentration in the substrate part of our sample. We suggest that the energy states giving rise to the H_{1T} and H_{2T} PLE peaks at approximately 9.4 meV above the H_1 and H_2 no-phonon lines are of the same type as the H_{3T} state in the case of the H_3-BE. The H_{5T} PLE line appears at 7.3 meV above the H_5 line. We propose that this transition is the same as the one giving rise to the H_{5T} PL line, reported to be 7.4 meV above the H_5 line.[2]

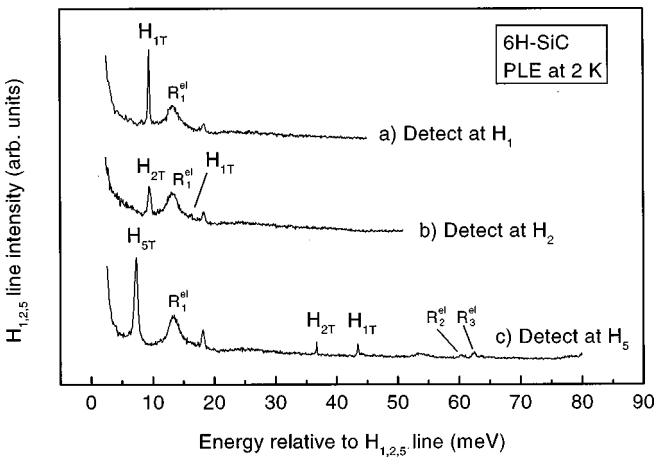

FIG. 3. The PLE spectra of the H_1-, H_2-, and H_5-BE's in 6*H*-SiC. The PL was monitored at the H_1, H_2, and H_5 no-phonon lines at 2 K. The PLE peaks are labeled H_{1T}, H_{2T}, and H_{5T}. The other peaks in the spectra are Raman peaks.

The H_2 PLE spectrum contains a weak peak at the H_{1T} position and the H_5 PLE spectrum contains peaks at both the H_{2T} and H_{1T} positions (see Fig. 3). This may be due to either the overlap of phonon-assisted emission from the higher-energy H-BE's with the lower-energy H-BE no-phonon lines, or energy transfer between the different sites. The absence of the H_1 and H_2 lines in the PLE spectra is a consequence of their low oscillator strength.

Figure 4 shows the PLE spectrum detected at the strong H_3 no-phonon line. In Fig. 4(a) the PL was excited with $\bar{E}\perp\bar{c}$ polarized light, and in Fig. 4(b), $\bar{E}\|\bar{c}$ polarized light was used. In the latter case the excitation was introduced through a cleaved edge of the sample. Due to the scattering and in-

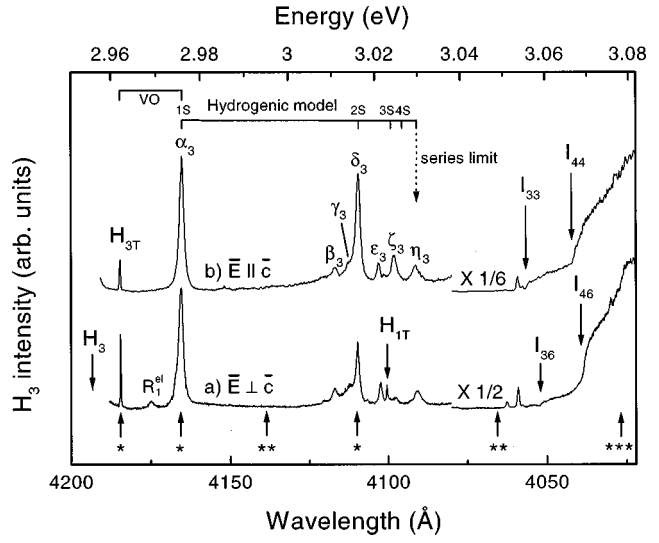

FIG. 4. The PLE spectrum of the H_3-BE in 6*H*-SiC. The PL was monitored at the H_3 no-phonon line at 2 K. In (a) the PL was excited with $\bar{E}\perp\bar{c}$ polarized light and in (b) $\bar{E}\|\bar{c}$ polarized light was used. Arrows marked*, **, and *** indicate excitation energies used in H_3-PL quenching experiments.

ternal reflections of light inside the sample, however, the polarization is expected to be only approximate. Thus, the spectra may also contain some contribution from the opposite polarization. In the rightmost part of the two spectra we observe clearly the steplike absorption edge due to the creation of free excitons with the assistance of momentum-conserving lattice phonons. The absorption edge in 6*H*-SiC has previously been detected by absorption measurements (see Ref. 10 and references therein) and PLE measurements of the free-exciton emission.[11] Steps related to the 36- and 46-meV $\overline{E}\perp\overline{c}$ phonons are observed in Fig. 4(a) (I_{36} and I_{46}), whereas in Fig. 4(b) we observe steps due to the 33- and 44-meV $\overline{E}\|\overline{c}$ phonons (I_{33} and I_{44}). The unlabeled peaks appearing just below the absorption edge in Figs. 4(a) and 4(b), as well as the R_1^{el} peak (same as in Fig. 3), are Raman peaks. We also measured the $\overline{E}\perp\overline{c}$ PLE spectra of the phonon replicas at 81 and 369 meV from the H_3 no-phonon line. In this case it was possible also to scan the excitation over the H_3 no-phonon line. These spectra are identical to the spectrum of the H_3 no-phonon line except for the shift of the Raman peaks and a very weak peak at the H_3 line position. The low intensity of the H_3 peak is consistent with the low oscillator strength found from PL measurements.[2] The H_{3T} PLE peak in Fig. 4 appears at approximately 6.2 meV above the no-phonon line. We suggest that this transition is the same as the one giving rise to the H_{3T} PL line, reported to be 6.5 meV above the H_3 line.[2] When the excitation is scanned across the H_{3T} line with high resolution, that is, with a small wavelength increment of the laser, it is clearly observed that the line is composed of two components. Their intensity ratio is approximately $\frac{1}{4}$ and their spacing is 0.37 meV. These are the NA and *A* components of the H_{3T} line. Both components are observed since the resolution at the detection side is only 0.6 meV as mentioned previously.

Similar to the PLE spectra of the H_2 and H_5-BE's, a peak at the H_{1T} line position is observed in the H_3 PLE spectrum [see Fig. 4(a)]. There is also a peak, labeled δ_3 in the figure, appearing at approximately the same position as the H_{2T} line. However, since the δ_3 peak is much stronger than the H_{1T} peak, it is unlikely that it is due only to H_{2T}. We thus consider at least part of its intensity to be due to absorption into an excited state of the H_3-BE. In addition to δ_3 we also attribute the peaks labeled α_3, β_3, γ_3, ε_3, ζ_3, and η_3 in Fig. 4 to absorption into excited states of the H_3-BE. The observed spectrum of excited states is similar for the $\overline{E}\perp\overline{c}$ and $\overline{E}\|\overline{c}$ polarizations [see Figs. 4(a) and 4(b)]. Apart from a slight shift (<0.5 meV) of the ε_3, ζ_3, and η_3 peaks to lower energy in the $\overline{E}\|\overline{c}$ spectrum, the peaks appear at the same energy positions in the two spectra. The relative intensities of the lines show that the δ_3 and ζ_3 peaks are preferably excited with $\overline{E}\|\overline{c}$ light, whereas $\overline{E}\perp\overline{c}$ polarization favors H_{3T} and H_{1T}. The energies of all the PLE peaks discussed above can be found in Table I.

B. Interpretation of the PLE results

Magneto-optical studies of the primary H_1, H_2, and H_3 no-phonon lines show that they have triplet character, whereas the H_{3T} no-phonon line does not split.[5] This has been explained by BE recombination at an isoelectronic center, the hole behaving as a spinlike particle due to strong localization.[5] The exchange interaction between the spin one-half hole and spin one-half electron splits the exciton state into a triplet and a singlet, the triplet appearing at lower energy. The transition from the triplet state to the crystal ground state is forbidden whereas the transition from the singlet state is allowed. The H_{3T} singlet has a higher oscillator strength compared to the H_3 triplet in approximate agreement with the above-mentioned selection rule.[2]

In light of these results, the neutral isoelectronic defect can be considered as hole attractive. The local defect potential localizes a hole and the charged hole in turn binds an electron in its Coulomb potential. This type of BE is sometimes called a pseudodonor BE. We propose to explain the H_{3T}, α_3, β_3, γ_3, δ_3, ε_3, ζ_3, and η_3 peaks in the H_3 PLE spectrum in terms of the ground and excited states of a weakly bound electron in a pseudodonor BE.

In general, the excitation spectrum of a BE can be obtained either by observing transitions from the crystal ground state to the ground and excited BE states, as is the case in this paper, or by observing transitions from the BE ground state to its excited states.[12] The latter case is similar to a conventional donor or acceptor absorption measurement, except that it requires an excitation beam to maintain a steady population of BE's. The selection rule for the creation of excitons requires that they be created in even-parity states. Therefore, the first method is expected to give information only on even-parity states. The second method, on the other hand, reveals transitions from even-parity ground states to odd-parity excited states. By comparing excitation spectra for the same BE obtained by the two different methods, it was found that the selection rule for the creation of excitons was not strictly obeyed.[12] Thus it may be possible to observe also transitions to odd-parity states when creating excitons. These are expected to be weak, however.

As mentioned earlier, the H-BE states are split into spin triplets and singlets due to the electron-hole exchange interaction. The transition to the H-BE ground-state triplet is very weak, and the same should apply for the excited states. We thus expect to see primarily transitions into *S*-like spin singlet states in the H-BE PLE spectra.

Shallow donor states in semiconductors are usually modeled by effective-mass theory (EMT). For semiconductors such as SiC which have multiple equivalent conduction-band minima, the reduction of degeneracy due to valley-orbit (VO) splitting (largest in the 1*S* ground state) also needs to be taken into account. Information concerning the states of shallow donors in SiC is scarce. The only donor that has been studied in any detail is the carbon site nitrogen donor (N_C). The excitation spectrum of the N_C donor has been obtained by infrared absorption measurements for a number of different SiC polytypes.[13–16] For the cubic polytype, 3*C*-SiC, the excitation spectrum has also been obtained by observing two-electron satellites of the N-BE luminescence.[17] Apart from the 1*S* ground state, the results for 3*C*-SiC are in good agreement with the predictions of EMT (calculations of Faulkner)[18] and are consistent with the electron effective mass determined by optically detected cyclotron-resonance (ODCR) measurements.[13] The 1*S* state is split by VO splitting into two states, an A_1 singlet and an *E* doublet (neglecting spin degeneracy) separated by approxi-

mately 8 meV, the A_1 state appearing at lower energy. For the other polytypes, comparison with theory is far more difficult, due to both the lack an appropriate EMT for these more complicated crystals and the less reliable data. Some attempts have been made, however,[14,15] but with limited success (see, e.g., discussion in Refs. 19 and 20).

Due to the lack of an adequate theory, support for our pseudodonor model for the primary H-BE's in 6*H*-SiC relies mainly on the qualitative similarity between the primary H-BE PLE spectra and known donor absorption spectra in 6*H*-SiC. 6*H*-SiC has six equivalent conduction-band minima, occurring along the *M*-*L* lines in the Brillouin zone.[21] VO splitting is expected to split the 1*S* ground state of a substitutional donor into two A_2 singlet states and two *E* doublet states, neglecting spin (here A_2 and *E* denote irreducible representations of the C_{3V} point group of a substitutional donor in 6*H*-SiC). Experimentally, the 1*S* ground state of the N_C donor in 6*H*-SiC is only seen to split into two states, however, the state lower in energy being an A_2 state. The size of the VO splitting is found to be very different for the different inequivalent substitutional sites. From absorption measurements[14] the VO splitting at the hexagonal site in 6*H*-SiC is found to be 12.6 meV (Raman measurements give 13.0 meV).[9] The VO splitting at the two cubic sites has not been determined by absorption measurements, but peaks in Raman spectra indicate values of 60.3 and 62.6 meV for these sites[9] (the three Raman lines mentioned here are the same as the R_1^{el}, R_2^{el}, and R_3^{el} lines observed in Fig. 3). The N_C donor ionization energies at the different sites are also different, 81.0 meV for the hexagonal site but 137.6 and 142.4 meV for the cubic sites.[14] The separation between the H_{3T} peak and the α_3 peak in the H_3 PLE spectrum is 13.8 meV. On the other hand, we do not observe any α peaks in the H_1 and H_2 PLE spectra. Since the H_1 and H_2 lines are much closer to the FEAE than the H_3 line, their PLE spectra span a narrower energy range than the H_3 PLE spectrum. But even so, the spectra show that the α state of the H_1-BE must be more than 35 meV above the H_{1T} state, and the α state of the H_2-BE more than 45 meV above the H_{2T} state. If we assume the H-BE behaves as a pseudodonor, it is natural to assign the separation between the H_3 and α_3 peaks to the electron VO splitting. In analogy with the N_C donors, we can then explain the apparently large VO splitting in the case of the H_1 and H_2-BE's by associating them with the two cubic sites, and consequently the H_3-BE with the hexagonal site. One would expect most of the peaks β_3, γ_3, δ_3, ε_3, ζ_3, and η_3 to be due to higher-order *S* states (2*S*, 3*S*, etc.) of the electron. However, as mentioned above, some of the weaker peaks might be due to transitions into odd-parity states since the selection rule is usually not perfectly obeyed. In Fig. 4 we show the energies of 3*S* and 4*S* states calculated from a simple hydrogenic model, assuming the α_3 and δ_3 peaks represent the 1*S* and 2*S* states, respectively (the VO splitting is here assumed to lower the energy of one of the two 1*S* states but leave the other one unchanged). The 3*S* state coincides with the ζ_3 peak but no line is seen at the position of the 4*S* state. In 6*H*-SiC the effective-mass tensor has three independent components.[22] This means that the 2*P*, 3*P*, etc. states are split into three levels each. Therefore, if excitation into *P* states can occur, then three extra peaks are expected in the vicinity of the 2*S* level. This might explain the weak β_3, γ_3, and ε_3 peaks. Similar arguments hold for higher-order *S* states, but the separation between the lines decreases rapidly with the order and will thus become more difficult to resolve.

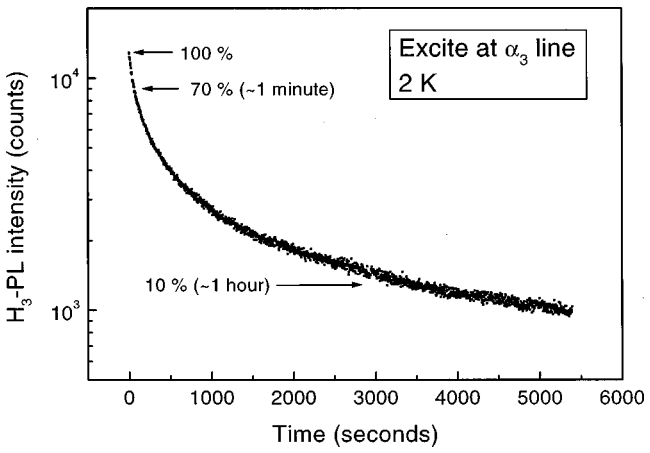

FIG. 5. Decay of the H_3-PL with time at 2 K during resonant optical excitation of H_3-BE's at the energy of the α_3 PLE peak (see Fig. 4).

Finally, we comment on the PLE spectrum of the secondary H_5-BE. Although this spectrum reaches 80 meV above the H_5 line, no excited states of the H_5-BE apart from the H_{5T} state are observed (see Fig. 3). The most likely explanation for this is a low transition probability (i.e., the peaks are too weak to be observed).

C. Quenching of the H-PL

The quenching experiments were performed by monitoring the H-PL (after cooling the sample from room temperature to 2 K in darkness) at the position of the strongest no-phonon line, H_3, as a function of time while exciting with laser light at various different energies. Although the quenching of the PL associated with the different H-BE's differs, it is believed that the underlying process is the same in all cases.[6] In the REDR model the variations may be explained by differences in the height of the potential barriers to the neighboring sites.[6]

Three types of quenching experiments were performed. (i) The H_3-PL was monitored as a function of time while exciting resonantly at the α_3, H_{3T}, or δ_3 position (indicated by * arrows in Fig. 4). The behavior was similar in all the three cases. Figure 5 shows the H_3-PL quenching in the case of excitation at the α_3 position. The H_3 signal is reduced to approximately 8% of its original intensity after 90 min of excitation. (ii) The H_3-PL was monitored while going through a sequence of different excitation energies. First, the H_3-PL was excited at the α_3 position for 1 min. During this time the signal decreased to approximately 70% of its initial value (see Fig. 5). The wavelength of the excitation was then changed to an off-resonant value (wavelength not coinciding with the position of any of the PLE peaks in Fig. 4) below the FEAE and kept there for 1 h. The wavelength was then changed back to the α_3 position. The H_3-PL immediately before and after the off-resonant excitation was the same, showing that the quenching during off-resonant excitation is negligible. The experiment was repeated for several different

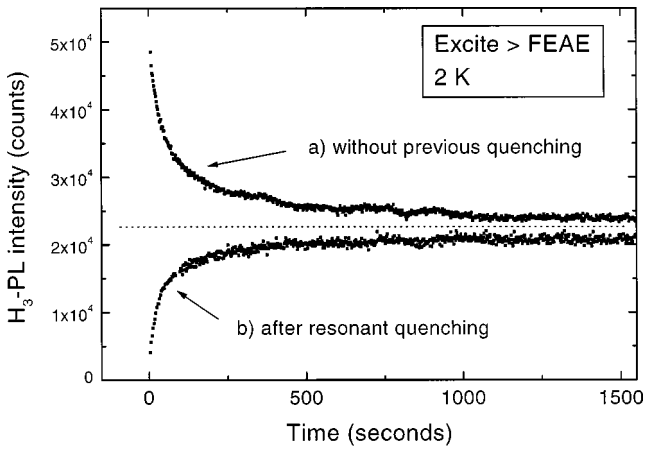

FIG. 6. Decay of the H_3-PL with time at 2 K during laser excitation above the FEAE, (a) without previous illumination, (b) after resonant excitation. The slight fluctuations in the curves are due to instabilities in the laser excitation.

off-resonant wavelengths (two examples of such wavelengths are indicated by ** arrows in Fig. 4). Also, a similar experiment where the α_3 excitation was blocked for 1 h instead of changing the wavelength gave the same result. (iii) The H_3-PL was monitored while exciting with light with an energy above the FEAE (indicated by a *** arrow in Fig. 4). In one case, this was done without any previous illumination (curve *a* in Fig. 6). In another case (curve *b* in Fig. 6), the H_3-PL had been quenched to below 10% of its initial value by using excitation at the α_3 position during 90 min (Fig. 5) prior to the excitation above the FEAE. The two curves, *a* and *b*, appear to approach the same steady-state value (indicated by a dotted line in Fig. 6) at approximately 45% of the peak intensity of the upper curve. In the experiment giving rise to curve *b* in Fig. 6, the effect of returning the excitation energy back to the α_3 position after 1 h of excitation above the FEAE was also investigated. The intensity of the H_3-PL immediately after the return was approximately five times larger than it had been after the initial quenching (before changing to above-FEAE excitation). This agrees with the rise observed in curve *b* of Fig. 6. The increase of the H_3-PL induced by the excitation above the FEAE is quenched by continuing the α_3 excitation.

Figure 5 shows that the quenching of the H-PL is nonexponential. This does not, however, rule out the possibility that the quenching of the H defect follows a first-order process. The reason lies in the way the experiment was performed. The quenching rate of the H-PL depends on the intensity of the excitation (the higher the intensity, the faster the quenching). In order to quench the PL signal within a reasonable period of time with the laser power we had at our disposal (10–25 mW depending on the wavelength), the laser spot needed to be focused onto the sample. The spot size was approximately 0.01 cm^{-2}. The detected PL contains contributions from different regions of the laser spot (not only the central part). The excitation intensity under the central part of the laser spot is higher than at positions off the center. This also means that the quenching rate is not constant over the excited area (since the excitation intensity is not). The detected decay of the H-PL may thus consist of a fast initial decay coming from the quenching of the H defect within the high-intensity central region of the laser spot, followed by a slow tail, coming from the off-central part where the intensity and hence the quenching are much slower.

D. Interpretation of the quenching results

The results presented in the preceding subsection can be explained by the existence of two forms of the H defect, one stable and the other metastable. Let us call the stable form *A* and the metastable form *B*. *A* gives rise to PL (the H-PL), whereas *B* does not (at least not within the energy region spanned by our PL measurements). Optical excitation may leave the defect unchanged or transform it from one form to the other ($A \rightarrow B$ or $B \rightarrow A$). The creation of a FE or the creation of a BE at *A* by resonant excitation can give rise to the $A \rightarrow B$ process. The creation of a FE can also give rise to the $B \rightarrow A$ process. When creating BE's resonantly at H defects in the *A* form (e.g., by exciting at the α_3 position), the $B \rightarrow A$ process is not active. This type of excitation can therefore convert all the *A*-form defects that are excited into *B*-form defects (within the time limits shown in Fig. 5, more than 90% are converted). The situation is different when FE's are created since in that case both the $A \rightarrow B$ and the $B \rightarrow A$ processes are active. If all the H defects are initially in the *A* form (as they are after cooling from room temperature in darkness), the above-FEAE excited H-PL (due to *A*) will be reduced until there are sufficiently many H defects in the *B* form to allow the $B \rightarrow A$ process to compensate for the $A \rightarrow B$ process (curve *a* in Fig. 6). On the other hand, if most of the H defects have been converted to the *B* form by resonant excitation before the above-FEAE excitation starts (curve *b* in Fig. 6), then the $B \rightarrow A$ process may dominate over the $A \rightarrow B$ process in the beginning, leading to an increase of the PL associated with the *A* form. As more and more of the defects are converted back to the *A* form, the importance of the $A \rightarrow B$ process increases, until it balances out the $B \rightarrow A$ process.

We now consider the nature of the two forms *A* and *B*. We consider two alternatives. The first is that they are different charge states of the H defect. The second is that they represent two configurations of the same charge state of the H defect. In order to change the charge state of the defect, an electron must be released or captured. The $A \rightarrow B$ process occurs very efficiently when BE's are formed at the H defects by resonant excitation. This type of excitation might lead to electron release or capture in two ways, either by an Auger process during the BE recombination or by an excitation of the defect independent of the BE formation. We immediately reject the latter alternative, however, since it is very difficult to explain why the quenching in that case should be active only at excitation energies corresponding to resonant BE formation. In order for an Auger process to take place, there needs to be an extra electron or hole present in the vicinity of the BE. This is the case, e.g., for BE's at donors and acceptors and is found to lead to short decay lifetimes for the associated PL.[23] However, experimental evidence [e.g., the long decay lifetime of the H-PL (Ref. 2)] indicates that the H defect is isoelectronic and thus does not have any extra electrons or holes to take part in an Auger process. It is thus very unlikely that an Auger process can occur during the recombination of the H_3-BE's. From the

above considerations, we conclude that a change of charge state is not a plausible explanation for the quenching of the H-PL. We are led to the model of two configurations of the same charge state. The $A \rightarrow B$ process needs a BE on the defect. The same seems to apply to the $B \rightarrow A$ process since FE's are needed in order to activate it. Either the presence of the BE's at the defects or their recombination gives rise to the transformation. Due to the properties of the H- and D-PL discussed in the Introduction, we find the latter alternative far more likely than the former.

IV. SUMMARY

Photoluminescence excitation properties of H-BE's in 6*H*-SiC have been investigated. In the case of the primary H-BE's, the PLE spectra reveal several excited states that have not been observed previously. In order to explain these states, we have proposed a pseudodonor model. The primary H-BE's are thus regarded as donors where strongly localized holes serve as the positive cores. From a comparison between the PLE spectra of the three different primary H-BE's, corresponding to the three inequivalent substitutional lattice sites in 6*H*-SiC, we attempt to distinguish between the hexagonal and cubic sites.

The excitation dependence of the quenching of the H-PL at 2 K has also been studied. We find that the quenching of the H-PL requires BE's at the defects. When exciting with an energy above the FEAE, we observe different types of behavior depending on the initial conditions. If there has been no illumination prior to the creation of the FE's, the H-PL is reduced until steady state is reached at a certain fraction of the original intensity. On the other hand, if one starts by quenching the H-PL by exciting BE's at the defects resonantly, and then changes to excitation above the FEAE, the FE creation can lead to an initial increase of the H-PL and then saturation at a certain value. We argue that our results are best explained by the existence of two configurations of the same charge state of the H defect, a stable one: *A* (giving rise to the H-PL), and a metastable one: *B* (not revealed in the PL spectrum). Recombination of BE's at these two configurations can give rise to the transformations $A \rightarrow B$ and $B \rightarrow A$. The existence of the *B* configuration is revealed through the effect of the $B \rightarrow A$ process on the temporal changes of the H-PL. The most probable mechanism by which the BE induces the change in configuration is through vibrational excitation of the defect during recombination. The local vibrational energy helps the defect to overcome the barrier to the other configuration.

ACKNOWLEDGMENTS

Support for this work was provided by the Swedish Council for Engineering Sciences (TFR), the SSF program SiCEP, and ABB Corporate Research.

[1] W. J. Choyke and L. Patrick, Phys. Rev. Lett. **29**, 355 (1972).
[2] L. Patrick and W. J. Choyke, Phys. Rev. B **8**, 1660 (1973).
[3] L. L. Clemen, R. P. Devaty, W. J. Choyke, A. A. Burk, Jr., D. J. Larkin, and J. A. Powell, in *Proceedings of the 5th International Conference on Silicon Carbide and Related Materials*, edited by M. G. Spencer, R. P. Devaty, J. A. Edmond, M. Asif. Khan, R. Kaplan, and M. M. Rahman, IOP Conf. Proc. No. 137 (IOP, Bristol, 1994), p. 227.
[4] W. J. Choyke and L. Patrick, Phys. Rev. B **9**, 3214 (1974).
[5] W. J. Choyke, L. Patrick, and P. J. Dean, Phys. Rev. B **10**, 2554 (1974).
[6] P. J. Dean and W. J. Choyke, Adv. Phys. **26**, 1 (1977).
[7] W. J. Choyke and L. Patrick, in *Proceedings of the Eleventh International Conference on the Physics of Semiconductors* (PWN-Polish Scientific, Warsaw, 1972), p. 177.
[8] L. Patrick and W. J. Choyke, Phys. Rev. B **9**, 1997 (1974).
[9] P. J. Colwell and M. V. Klein, Phys. Rev. B **6**, 498 (1972).
[10] R. P. Devaty, W. J. Choyke, S. G. Sridhara, L. L. Clemen, D. G. Nizhner, D. J. Larkin, T. Troffer, G. Pensl, T. Kimoto, and H. S. Kong, in *Proceedings of the 7th International Conference on Silicon Carbide, III-Nitrides and Related Materials*, edited by G. Pensl, H. Morkoc, B. Monemar, and E. Janzén, Materials Science Forum Vols. 264–268 (Trans Tech, Aedermannsdorf, 1998), p. 455.
[11] I. G. Ivanov, T. Egilsson, A. Henry, and E. Janzén, Mater. Sci. Eng., B **61–62**, 265 (1999).
[12] D. Labrie, T. Timusk, and M. L. W. Thewalt, Phys. Rev. Lett. **58**, 81 (1984).
[13] W. J. Moore, P. J. Lin-Chung, J. A. Freitas, Jr., Y. M. Altaiskii, V. L. Zuev, and L. M. Ivanova, Phys. Rev. B **48**, 12 289 (1993); W. J. Moore, J. A. Freitas, Jr., Y. M. Altaiskii, V. L. Zuev, and L. M. Ivanova, in *Proceedings of the 5th International Conference on Silicon Carbide and Related Materials* (Ref. 3), p. 181; W. J. Moore, J. A. Freitas, Jr., and P. J. Lin-Chung, Solid State Commun. **93**, 389 (1995).
[14] W. Suttrop, G. Pensl, W. J. Choyke, R. Stein, and S. Leibenzeder, J. Appl. Phys. **72**, 3708 (1992).
[15] W. Götz, A. Schöner, G. Pensl, W. Suttrop, W. J. Choyke, R. Stein, and S. Leibenzeder, J. Appl. Phys. **73**, 3332 (1993).
[16] Th. Troffer, W. Götz, A. Schöner, W. Suttrop, G. Pensl, R. P. Devaty, and W. J. Choyke, in *Proceedings of the 5th International Conference on Silicon Carbide and Related Materials* (Ref. 3), p. 173.
[17] P. J. Dean, W. J. Choyke, and L. Patrick, J. Lumin. **15**, 299 (1977).
[18] R. A. Faulkner, Phys. Rev. **184**, 713 (1969).
[19] W. M. Chen, N. T. Son, E. Janzén, D. M. Hofmann, and B. K. Meyer, Phys. Status Solidi A **162**, 79 (1997).
[20] R. P. Devaty and W. J. Choyke, Phys. Status Solidi A **162**, 5 (1997).
[21] C. Persson and U. Lindefelt, J. Appl. Phys. **82**, 5496 (1997).
[22] F. Engelbrecht, S. Huant, and R. Helbig, Phys. Rev. B **52**, 11 008 (1995).
[23] J. P. Bergman, O. Kordina, and E. Janzén, Phys. Status Solidi A **162**, 65 (1997).